*The definitive version was published in Science, **2023**, 379, 494-499, DOI: 10.1126/science.ade8190.*

https://science.org/doi/10.1126/science.ade8190

Asymmetric Counteranion Directed Photoredox Catalysis

Sayantani Das[1†], Chendan Zhu[1†], Derya Demirbas[1], Eckhard Bill[2¥], Chandra Kanta De[1*] and Benjamin List[1*]

[1]Max-Planck-Institut für Kohlenforschung, Kaiser-Wilhelm-Platz 1, D-45470 Mülheim an der Ruhr, Germany.

[2]Max-Planck-Institut für Chemische Energiekonversion, Stiftstrasse 34–36, D-45470 Mülheim an der Ruhr, Germany.

*Corresponding author. Email: list@kofo.mpg.de

†These authors contributed equally to this work. ¥Deceased October 6th 2022.

Abstract: Photoredox catalysis enables unique and broadly applicable chemical reactions but controlling their selectivity has proven to be difficult. The pursue of enantioselectivity is a particularly daunting challenge, arguably due to the high energy of the activated radical(ion) intermediates, and previous approaches have invariably required pairing of the photoredox catalytic cycle with an additional activation mode for asymmetric induction. A potential solution to photoredox reactions proceeding via radical ions would be the catalytic utilization of enantiopure counterions. However, while attempts toward this approach have been described, high selectivity has not yet been accomplished. Here we report a potentially general solution to radical cation-based asymmetric photoredox catalysis. We describe organic salts, featuring confined IDPi counteranions that catalyze highly enantioselective [2+2]-cross cycloadditions of styrenes.

One-Sentence Summary: Organic salts, featuring enantiopure counteranions, efficiently catalyze radical cation-based asymmetric photoredox reactions.

Main Text: Photoredox catalysis is an emerging field in chemistry, enabling the design and development of diverse transformations that often complement the traditional toolkit of chemical synthesis (1). Typically, in a photoredox transformation, light is absorbed by the photocatalyst, which then triggers a single electron transfer (SET) event, leading to the formation of highly reactive radical ions. For example, in an oxidative mode, SET delivers the corresponding substrate radical cation. In contrast, in a reductive mode, a radical anion is initially generated via SET from the catalyst to the substrate. Both pathways have led to the design of a large diversity of different and often broadly useful transformations (2–5). As a consequence, the development of asymmetric photoredox catalysis (6) became a topic of high current relevance. However, since general enantioselective methods toward the control of radical(ion)s per se have not been available, previous approaches to asymmetric photoredox catalysis invariably required a second activation mode and catalytic cycle to enable the stereoselective bond forming event (Figure 1A). Examples include enamine (7) and iminium ion catalysis (8), carbene catalysis (9), Brønsted acid catalysis (10–12), transition metal catalysis (13–16), and Lewis acid catalysis (17–21), which all benefit from previously established methods of asymmetric induction. While these dual catalysis approaches have led to useful transformations with excellent enantioselectivity, the requirement of a second catalytic cycle, even in those cases when only a single catalyst is used, creates certain limitations with regard to substrate functionalization and, more importantly, to reaction diversity in general. Approaches not in need of such a second catalytic cycle could potentially offer a more general solution to asymmetric photoredox catalysis and enable enantioselective versions of a multitude of broadly useful methods for chemical synthesis.

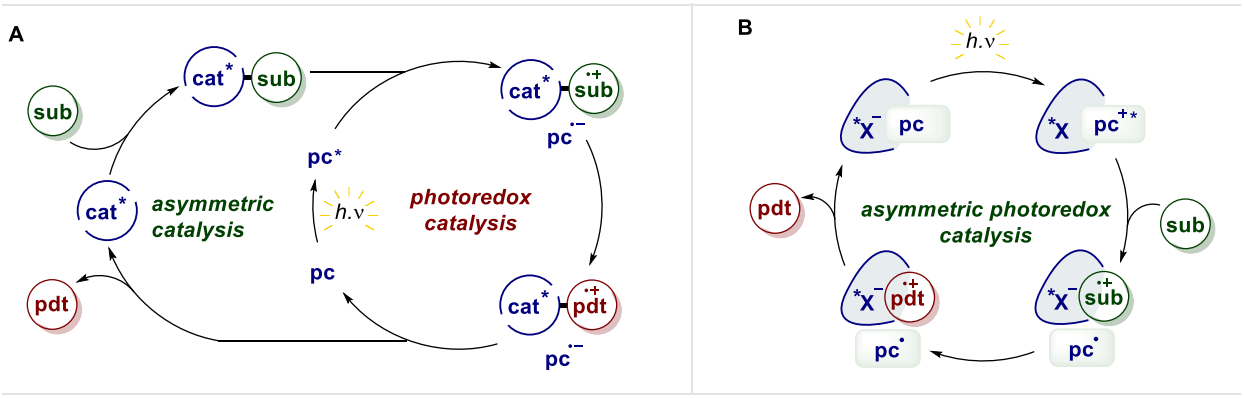

Figure 1: (A) Previous approaches to highly enantioselective photoredox catalysis have been based on two catalytic cycles, a photoredox cycle and an asymmetric catalysis cycle. (B) Suggested approach here. sub = substrate; cat = catalyst; pdt = product; pc = photocatalyst.

One particularly promising and elegant recent approach employs (modified) enzymes (22), which by virtue of their well-defined active sites, can pre-organize highly reactive intermediates to engage in stereoselective transformations. An alternative strategy involves the utilization of enantiopure counterions, paired with an achiral, charged photocatalyst. Recently, attempts toward this approach in radical cation-based Diels–Alder reactions (23) and in anti-Markovnikov hydroetherifications (24) have been reported. However, the employed chiral, binol-based phosphates did not provide high enantioselectivity. We hypothesized that in order to advance this asymmetric counteranion-directed catalysis (ACDC) (25) approach to photoredox catalysis toward greater selectivity and generality, two features of the enantiopure counteranion would be required. First, its basicity should not be too high to avoid deprotonation of the typically highly acidic radical cation intermediates, which could lead to nonproductive radical pathways. The second important anion-feature we expected to be required would be a confined active site, capable of controlling the selectivity in reactions of only weakly coordinating radical cations. Indeed, we were hopeful that our recently introduced imidodiphosphorimidiate (IDPi) (26) anions, which have enabled control over other challenging and previously inaccessible cations, such as aliphatic oxocarbenium ions (27) and even purely hydrocarbon-based carbocations (28), could offer a solution in this context. Such an ACDC approach to photoredox catalysis, by only requiring a single catalytic cycle, could offer great potential generality (Figure 1B). Minimal and sufficient requirement of this strategy would only be the formation and involvement in the stereoselectivity determining step of a radical cation intermediate.

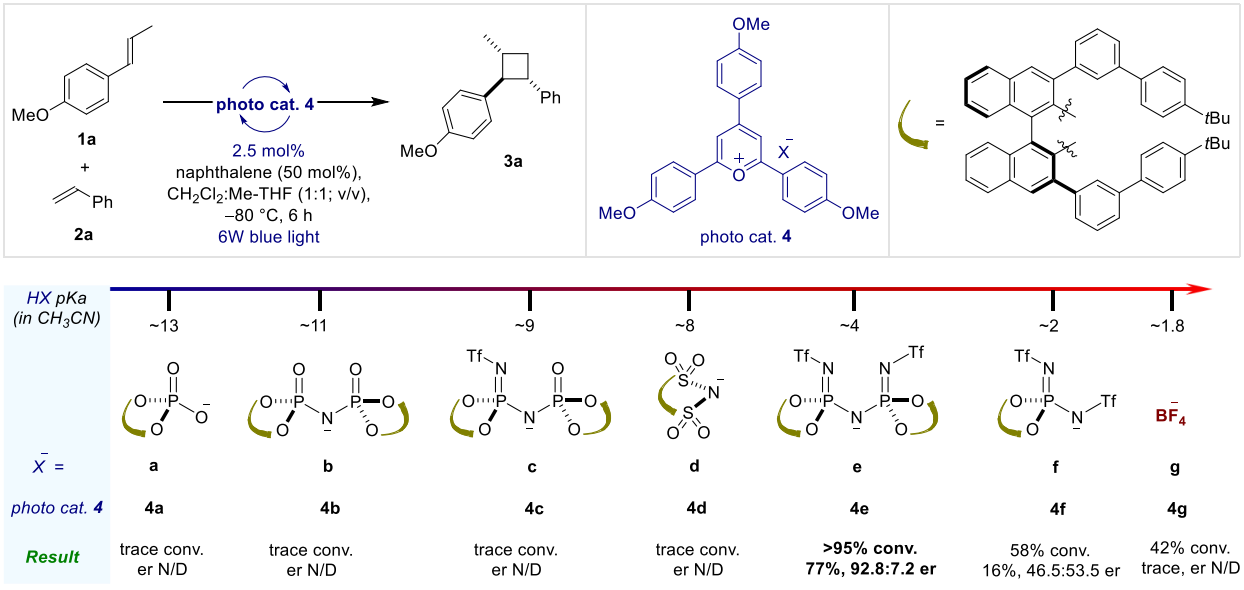

Figure 2: Investigation of different counteranions in the pyrylium photoredox catalytic intermolecular [2+2] cycloaddition reaction between *trans*-anethol and styrene. Yields were determined by ^{1}H Nuclear Magnetic Resonance (NMR) Spectroscopy using benzyl methyl ether as internal standard. The er was determined by HPLC.

At the onset of our study we decided to explore the photoredox catalytic intermolecular [2+2] cycloaddition reaction between *trans*-anethol and styrene. Despite pioneering contributions on enantioselective photocatalytic [2+2] cycloadditions (29, 30), this challenging and potentially useful reaction has not previously been accomplished enantioselectively. We began by exchanging the counteranion of the commercially available pyrylium tetrafluoroborate photoredox catalyst **4g** with a series of enantiopure anions, derived from acids covering a broad pKa range (Figure 2, see the SI for details). As expected the conjugate base of a chiral phosphoric acid (CPA; **a**) and an imidodiphosphoric acid (IDP; **b**) were too basic to impart any reactivity. Similar results were observed when using anion of an iminoimidodiphosphoric acid (iIDP; **c**) and a chiral disulfonimide (DSI; **d**). In sharp contrast, the anion of our highly acidic and confined imidodiphosphorimidate (IDPi; **e**), catalyst **4e** enabled superior catalytic performance. More importantly, high enantioselectivity was already observed with this pyrylium-IDPi salt. Interestingly, the anion of the even stronger phosphoramidimidate (PADi; **f**) afforded the product in only moderate yield and poor enantioselectivity. While 58% consumption of substrate **1a** was observed, only 16% yield of product **3a** was obtained with poor enantioselectivity, presumably due to a lack of confinement. Parent tetrafluoroborate catalyst **4g** gave a moderate conversion of substrate **1a** but provided only traces of the product. Upon a brief screening of catalysts and reaction conditions (see SI for details) we selected catalyst **4e** and a 1:1 solvent mixture of dichloromethane and 2-methyltetrahydrofuran at –100 °C for further study and found that cycloaddition product **3a** can be obtained in excellent yield and with excellent enantioselectivity (95.5:4.5 er).

A broad range of styrenes with different electronic property and substituents at different ring positions were evaluated and the cyclobutane products were obtained with good to excellent yields and enantioselectivities. Styrenes with electron withdrawing substituents gave products **3b**–**3f** in good yields and with good to excellent enantioselectivities. Similarly, styrenes featuring electron donating substituents, apparently independent of their steric properties, provided products **3f**–**3i** in excellent enantioselectivities. Disubstituted arene-based styrenes were also found to be suitable reaction partners and furnished the desired products (**3j**–**3k**) with excellent enantioselectivity.

Remarkably, the reaction tolerates different functional groups, including an alcohol, a silyl ether, an aldehyde, an ester and even a terminal olefin, leading to products **3l**–**3p** in good yield and with excellent enantioselectivities. We also investigated two other anethol derivatives providing benzyl ether **3q** and free phenol **3r** with excellent enantioselectivity. For additional substrates, see the SI.

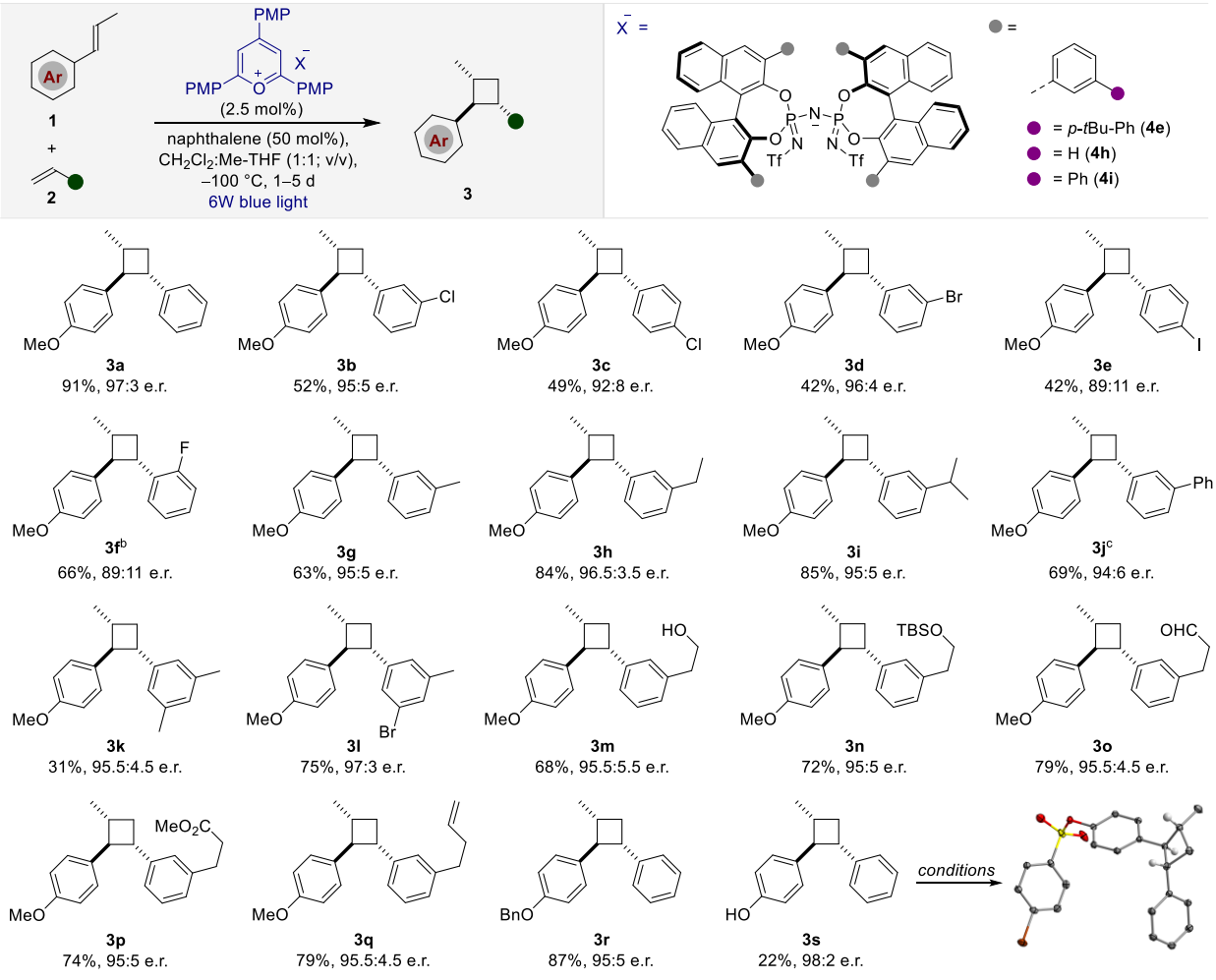

Figure 3: Scope of the intermolecular [2+2] cycloaddition reactions. Reactions were performed at 0.1 mmol scale. er was determined by HPLC (see SI for details). [b]Using catalyst **4h**. [c]Using catalyst **4i**.

Interestingly, as one would expect for a reaction proceeding via radical cation-IDPi anion pair, we found almost identical enantioselectivity when we used a variety of photocatalysts that feature an identical IDPi counteranion but that require irradiation with light of different wavelengths (Figure 4). For example, three different photoredox catalysts which are known to be excited with blue light were evaluated (**4e**–**6e**). All led to full consumption of olefin **1a**. However, while our standard

catalyst **4e** and the frequently used *N*-Ph acridinium organophotoredox catalyst **5e** led to the product in 90% and 56% yields and with identical enantioselectivities, popular iridium catalyst **6e** did not provide the desired product. Recently, several different organophotoredox catalysts that can be excited with green light were disclosed (31, 32) and we became interested in exploring these cationic species paired with our IDPi counteranion. Indeed, photoredox catalysts **7e** and **8e** upon green light irradiation, furnished the product in 92% and 19% yield respectively and with the same enantioselectivity. Finally, a ruthenium-based-photoredox catalyst **9e**, irradiated with white light furnished product **3a** in <5% yield and once again with the similar 97.3:2.7 er. The small changes of enantioselectivity may arise from the heat generated by the different light sources. The obtained results clearly support our ion pairing design and suggest generality of asymmetric counteranion directed photoredox catalysis (ACDPC).

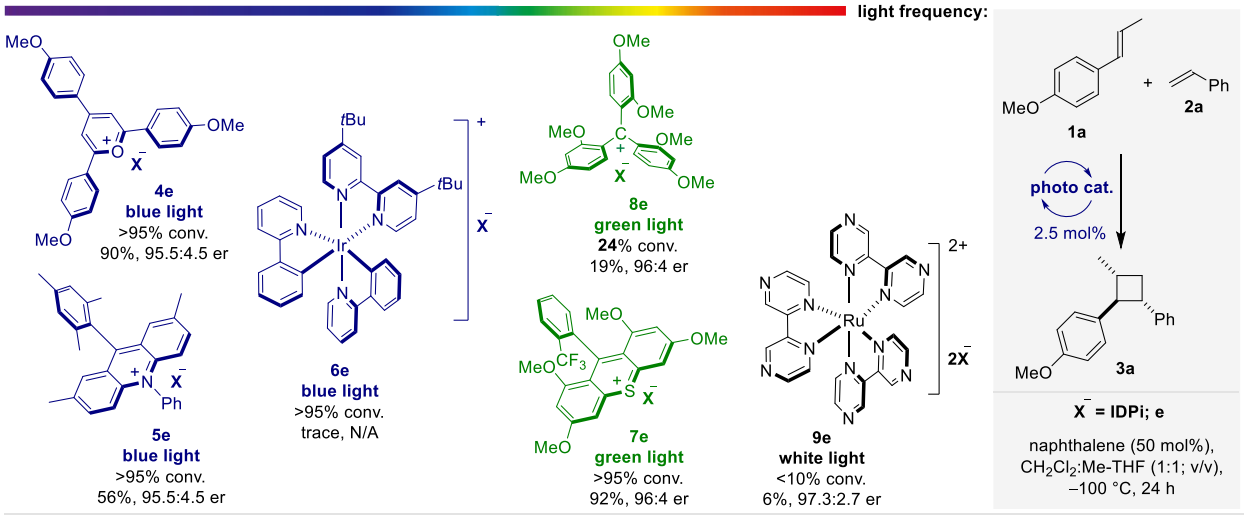

Figure 4: Evaluation of different photocatalysts with IDPi counteranion under different light wave length.

The availability of these enantiopure photocatalysts via simple salt metathesis enabled an evaluation of their chemical stability and photophysical properties. At first, to establish the stability of catalyst **4e**, our model reaction between *trans*-anethol and styrene was carried out under optimized conditions and the reaction mixture was analyzed by NMR spectroscopy after approximately 60% conversion. Indeed, both ^{19}F NMR (Figure 5A) and ^{31}P NMR (Figure 5B) spectra confirmed that essentially no decomposition took place. We further compared catalysts **4g** and **4e** by UV-vis absorption and fluorescence spectroscopy. As expected, both catalysts have very similar spectra in the visible range with λ_{max1} at 425 nm and λ_{max2} at 456 nm (Figure 5C, left part).

Similarly, upon excitation at 425 nm, identical fluorescence spectra with λ_{max} at 535 nm were measured for both catalysts (Figure 5C, right part). Our spectroscopic investigations thus confirm the stability of the pyrylium photocatalyst. Furthermore, in order to identify which reagent engages in the initial oxidative SET with the excited state catalyst, steady state fluorescence (33, 34) quenching experiments with the individual reaction components have been conducted. We have measured the steady state fluorescence decay for both catalysts **4g** and **4e**, respectively, using 425 nm pulsed excitation in the presence of starting materials **1a** or **2a**, respectively. As expected form the redox potential of catalyst **4g** (+1.84v *vs* SEC), anethol (**1a**, +1.14v *vs* SEC) showed a strong and concentration dependent fluorescence decay (Figure 5D). A very similar behavior was observed with catalyst **4e** (Figure 5E). In sharp contrast, neither catalyst **4g** nor catalyst **4e** showed any significant fluorescence decay with styrene **2a** (+1.97v *vs* SEC). The similar fluorescence quenching of catalysts **4g** (blue) and **4e** (orange) by substrate **1a** are further presented in Stern-Volmer plots (I_0/I *vs* conc. of **1a**) (Figure 5F).

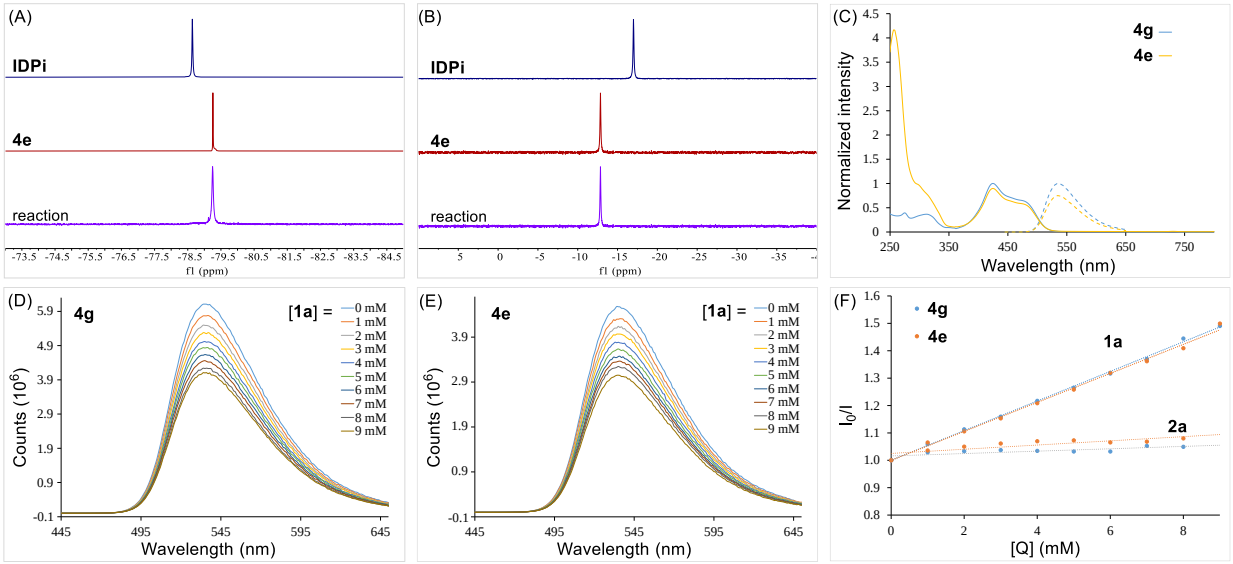

Figure 5: (A) ^{19}F NMR stacks. (B) ^{31}P NMR stacks. (C) UV-vis and fluorescence spectra of catalysts **4e** and **4g**. (D) Fluorescence quenching of catalyst **4g** with anethol (**1a**). (E) Fluorescence quenching of catalyst **4e** with anethol (**1a**). (F) Stern-Volmer plot of the fluorescence quenching of catalysts **4g** (blue) and for **4e** (orange) by substrates **1a** and **2a**.

Our results are consistent with the previously established catalytic cycle of the intermolecular [2+2] cycloadditions under photoredox catalysis or single electron Lewis acid conditions (35–38). Accordingly, photocatalyst **4e** is first converted into its excited state **4e*** upon blue light

irradiation. Excited catalyst **4e*** then accepts an electron from anethol (**1a**), rendering the corresponding radical cation **1a**$^{\bullet+}$ and the photocatalyst as radical species **A**. Intermediate **1a**$^{\bullet+}$ engages in subsequent and presumably stepwise C–C bond forming events furnishing radical cation intermediate **3a**$^{\bullet+}$. A single electron reduction of this intermediate will then give rise to product **3a**.

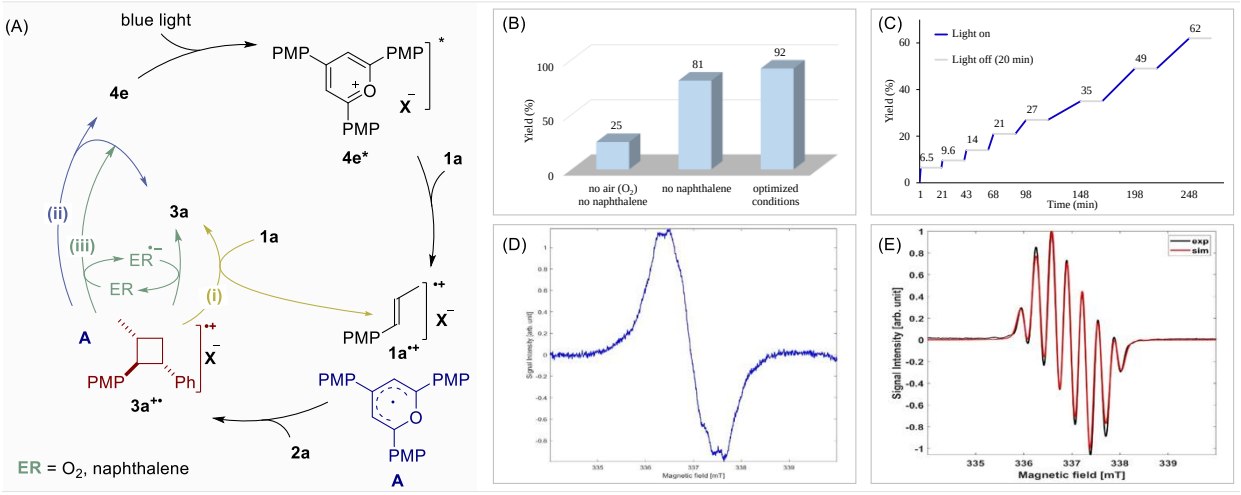

Figure 6: (A) Proposed catalytic cycle. (B) Results with or without electron relay (ER) catalysts naphthalene or oxygen. (C) Light on-off cycles. (D) EPR measurements of the reaction using catalyst **4e** at –83 °C and (E) EPR measurements of the reaction mixture using photocatalyst **5e** at –30 °C under continuous photoexcitation with blue light.

There are several possibilities of how this last SET step proceeds. Plausible pathways include (i) a propagation mechanisms in which substrate **1a** serves as electron donor toward radical cation intermediate **3a**$^{\bullet+}$, delivering reactive species **1a**$^{\bullet+}$ along with product **3a**; (ii) catalyst radical **A** could transfer an electron to product radical cation **3a**$^{\bullet+}$, to provide product **3a** while simultaneously regenerating photocatalyst **4e**, (iii) catalyst radical **A** could be oxidized by an electron relay catalyst, for example naphthalene, the reduction product of which would subsequently reduce radical cation **3a**$^{\bullet+}$, regenerating the electron relay catalyst while furnishing product **3a**. In this scenario, the role of the electron relay catalyst is to overcome the kinetic obstacle of step (ii), which requires the reaction of two highly reactive intermediates, each present in only small concentration.

To gain further insight into the catalytic cycle, EPR experiments were performed. First, the individual components of the reaction (solvent, reactants **1a** and **1b**, naphthalene, photocatalyst **4e**) in 1:1 dichloromethane:THF were irradiated under steady state condition separately with blue light at –83 °C in the spectrometer. As expected, no EPR signal was detected under either one of these conditions (see SI for details, SI Figure 2). However, a distinct EPR signal was observed when we investigated the entire reaction mixture (Figure 6D). While radical cation $\mathbf{1a}^{\bullet+}$ (35) could not be detected under these conditions, we hypothesize that the observed signal is due to the formation of catalyst radical **A**, consistent with a previously reported system (39). The cw X-band EPR spectra of **A** with g = 2.003 shows an isotropic and fast-motional of douplet radicals electron spin coupling. Additionally, to further support our hypothesis, *N*-Ph-acridinium photocatalyst **5e** was used in the EPR measurements. As expected, EPR spectra of *N*-Ph-acridinium photocatalyst with 10mW power and with modulation amplitude of 0.2 G shows seven hyperfine splitting lines (Figure 6E). The hyperfine coupling is presumably due to the *N*-Ph moiety of the catalyst, which is in agreement with the Easyspin simulated spectra with a_1(1H), a_2(1H), a_3(1H) (n=2 2 1) nuclei at g = 2.0034, A = (0.2751 0.3826 0.5909) and Lorentzian width (0.2503 0.0419). These experiments are consistent with the proposed SET from substrate **1a** to the excited state of the photocatalyst. Furthermore, since continuous light irradiation is needed to achieve full consumption of starting material **1a,** propagation pathway (i) cannot be the primary pathway to complete the catalytic cycle. This assumption is further supported by light on-off cycles. In the dark, no conversion was observed and progress of the reaction resumed in presence of light. Additionally, a time dependent continuous EPR signal intensity decay in the dark was observed when the reaction mixture was first irradiated with blue light at –83 °C in the EPR spectrometer for few minutes, after which the light was switched off (see SI for details, SI Figure 4). In order to support the role of the electron relay catalyst, control experiments were performed and summarized in Figure 6B. In absence of an ER catalyst (oxygen or naphthalene) an almost three fold rate deceleration was observed.

Asymmetric counteranion directed photoredox catalysis (ACDPC) offers a broadly useful and general approach to photoredoxcatalysis proceeding via all types of radical cations and wider utilization of the principles described here can be anticipated.

References and Notes

1. N. A. Romero, D. A. Nicewicz, Organic photoredox catalysis. *Chem. Rev.* **116**, 10075–10166 (2016).
2. T. P. Yoon, M. A. Ischay, J. Du, Visible light photocatalysis as a greener approach to photochemical synthesis. *Nat. Chem.* **2**, 527–532 (2010).
3. C. K. Prier, D. A. Rankic, D. W. C. MacMillan, Visible light photoredox catalysis with transition metal complexes: Applications in organic synthesis. *Chem. Rev.* **113**, 5322–5363 (2013).
4. D. M. Schultz, T. P. Yoon, Solar synthesis: Prospects in visible light photocatalysis. *Science* 343, 1239176 (2014).
5. R. Brimioulle, D. Lenhart, M. M. Maturi, T. Bach, Enantioselective catalysis of photochemical reactions. *Angew. Chem. Int. Ed.*, **54**, 3872–3890 (2015).
6. E. Meggers, Asymmetric catalysis activated by visible light. *Chem. Commun*. **51**, 3290–3301 (2015).
7. D. A. Nicewicz, D. W. C. MacMillan, Merging photoredox catalysis with organocatalysis: The direct asymmetric alkylation of aldehydes. *Science* **322**, 77–80 (2008).
8. J. J. Murphy, D. Bastida, S. Paria, M. Fagnoni, P. Melchiorre, Asymmetric catalytic formation of quaternary carbons by iminium ion trapping of radicals. *Nature* **532**, 218–222 (2016).
9. D. A. DiRocco, T. Rovis, Catalytic asymmetric α-acylation of tertiary amines mediated by a dual catalysis mode: N-heterocyclic carbene and photoredox catalysis. *J. Am. Chem. Soc.* **134**, 8094–8097 (2012).
10. L. J. Rono, H. G. Yayla, D. Y. Wang, M. F. Armstrong, R. R. Knowles, Enantioselective photoredox catalysis enabled by proton-coupled electron transfer: Development of an asymmetric aza-pinacol cyclization. *J. Am. Chem. Soc.* **135**, 17735–17738 (2013).
11. E. M. Sherbrook, M. J. Genzink, B. Park, I. A. Guzei, M-H. Baik, T. P. Yoon, Chiral Brønsted acid-controlled intermolecular asymmetric [2 + 2] photocycloadditions. *Nat. Commun*. **12**, 5735 (2021).
12. R. S. J. Proctor, H. J. Davis, R. J. Phipps, Catalytic enantioselective Minisci-type addition to heteroarenes. *Science* **360**, 419–422 (2018).
13. H. Huo, X. Shen, C. Wang, L. Zhang, P. Röse, L.-A. Chen, K. Harms, M. Marsch, G. Hilt, E. Meggers, *Nature* **515**,100–103 (2014).
14. L. Huan, X. Shu, W. Zu, D. Zhong, H. Huo, Asymmetric benzylic C(sp3)−H acylation via dual nickel and photoredox catalysis. *Nat. Commun*. **12**, 3536 (2021).
15. P. Zheng, P. Zhou, D. Wang, W. Xu, H. Wang, T. XU, Dual Ni/photoredox-catalyzed asymmetric cross-coupling to access chiral benzylic boronic esters. *Nat. Commun*. **12**, 1646 (2021).
16. J, Li, M. Kong, B. Qiao, R. Lee , X. Zhao, Z. Jiang, Formal enantioconvergent substitution of alkyl halides via catalytic asymmetric photoredox radical coupling. *Nat. Commun*. **9**, 2445 (2018).

17. M. P. Sibi, J. Ji, J. H. Wu, S. Gürtler, N. A. Porter, Chiral Lewis acid catalysis in radical reactions: enantioselective conjugate radical additions. *J. Am. Chem. Soc.* **118**, 9200–9201 (1996).

18. J. Du, K. L. Skubi, D. M. Schultz, T. P. Yoon, A dual-catalysis approach to enantioselective [2 + 2] photocycloadditions using visible light. *Science* **344**, 392–397 (2014).

19. H. Guo, E. Herdtweck, T. Bach, Enantioselective Lewis acid catalysis in intramolecular [2+2] photocycloaddition reactions of coumarins. *Angew. Chem. Int. Ed.* **49**, 7782–7785 (2010).

20. R. Brimioulle, T. Bach, Enantioselective Lewis acid catalysis of intramolecular enone [2+2] photocycloaddition reactions. *Science* **342**, 840–843 (2013)

21. X. Huang , T. R. Quinn , K. Harms , R. D. Webster , L. Zhang , O. Wiest, E. Meggers, Direct visible-light-excited asymmetric Lewis acid catalysis of intermolecular [2+2] photocycloadditions. *J. Am. Chem. Soc.* **139**, 9120–9123 (2017).

22. M. A. Emmanuel, N. R. Greenberg, D. G. Oblinsky, T. K. Hyster, Accessing non-natural reactivity by irradiating nicotinamide-dependent enzymes with light. *Nature* **540**, 414–417 (2016).

23. P. D. Morse, T. M. Nguyen, C. L. Cruz, D. A. Nicewicz, Enantioselective counter-anions in photoredox catalysis: The asymmetric cation radical Diels-Alder reaction. *Tetrahedron* **74**, 3266–3272 (2018).

24. Z. Yang, H. Li, S. Li, M-T Zhang, S. Luo, A chiral ion-pair photoredox organocatalyst:enantioselective anti-Markovnikov hydroetherification of alkenols. *Org. Chem. Front.* **4**, 1037–1041 (2017).

25. S. Mayer, B. List, Asymmetric counteranion-directed catalysis. *Angew. Chem. Int. Ed.* **45**, 4193–4195 (2006).

26. L. Schreyer, R. Properzi, B. List, IDPi Catalysis. *Angew. Chem. Int. Ed.* **58**, 12761–12777 (2019).

27. S. Lee, P. S. J. Kaib, B. List, Asymmetric catalysis via cyclic, aliphatic oxocarbenium ions. *J. Am. Chem. Soc.* **139**, 2156–2159 (2017).

28. R. Properzi, P. S. J. Kaib, M. Leutzsch, G. Pupo, R. Mitra, C. De, L. Song, P. R. Schreiner, B. List, Catalytic enantiocontrol over a non-classical carbocation. *Nat. Chem.* **12**, 1174–1179 (2020).

29. R. Alonso, T. Bach, A chiral thioxanthone as an organocatalyst for enantioselective [2+2] photocycloaddition reactions induced by visible light. *Angew. Chem. Int. Ed.* **53**, 4368–4371 (2014).

30. D. I. Schuster, G. Lem, N. A. Kaprinidis, New insights into an old mechanism: [2 + 2] photocycloaddition of enones to alkenes. *Chem. Rev.* **93**, 3–22 (1993).

31. K.Tanaka, M. Kishimoto, M. Sukekawa, Y. Hoshino, K. Honda, Green-light-driven thioxanthylium-based organophotoredox catalysts: Organophotoredox promoted radical cation Diels-Alder reaction. *Tetrahedron Lett.* **59**, 3361–3364 (2018).

32. L. Wang, Y. Xu, Q. Zuo, H. Dai, L. Huang, M. Zhang, Y. Zheng, C. Yu, S. Zhang, Y. Zhou, Visible light-controlled living cationic polymerization of methoxystyrene. *Nat Commun*. **13**, 3621 (2022)

33. V. Kottisch, Q. Michaudel, B. P. Fors, Cationic polymerization of vinyl ethers controlled by visible light. *J. Am. Chem. Soc*. **138**, 15535–15538 (2016).

34. Q. Michaudel, T. Chauviré, V. Kottisch, M. J. Supej, K. J. Stawiasz, L. Shen, W. R. Zipfel, H. D. Abruña, J. H. Freed, B. P. Fors, Mechanistic insight into the photocontrolled cationic polymerization of vinyl ethers. *J. Am. Chem. Soc.* **139**, 15530–15538 (2017).

35. J. H. Shin, E. Y. Seong, H. J. Mun, Y. J. Jang, E. J. Kang, Electronically mismatched cycloaddition reactions via first-row transition metal, iron(III)–polypyridyl Complex. *Org. Lett*. **20**, 5872–5876 (2018).

36. Y. Yu, Yu. Fua, F. Zhong, Benign catalysis with iron: facile assembly of cyclobutanes and cyclohexenes via intermolecular radical cation cycloadditions. *Green Chem*. **20**, 1743–1747 (2018).

37. K. Tanaka, Y. Iwama, M. Kishimoto, N. Ohtsuka, Y. Hoshino, K. Honda, Redox potential controlled selective oxidation of styrenes for regio- and stereoselective crossed intermolecular [2 + 2] cycloaddition via organophotoredox catalysis. *Org. Lett*. **22**, 5207–5211 (2020).

38. R. Li, B. C. Ma, W. Huang, L. Wang, D. Wang, H. Lu, K. Landfester, K.A. I. Zhang, Photocatalytic regioselective and stereoselective [2 + 2] cycloaddition of styrene derivatives using a heterogeneous organic photocatalyst. *ACS Catal*. **7**, 3097–3101 (2017).

39. P. S. Lakkaraju, D. Zhou, H. D. Roth, Oxidation and dehydrogenation of a phenol ether in a pentasil zeolite (Na ZSM-5): an EPR study. *Chem. Commun*. 2605–2606 (1996).

Acknowledgments: We are grateful to M. Leutzsch for his assistance with NMR spectroscopy, Marc Meyer and Harun Tüysüz for assistance with UV-vis and fluorescence spectroscopy and H. Zhou for her assistance with determining the absolute configuration by CD spectrometry. We would like to acknowledge the excellent support by the late Dr. Eckhard Bill, a renowned and leading expert in the field of EPR spectroscopy who will always be remembered for his outstanding contribution to science.

Funding:

Generous support from the Max Planck Society, the Deutsche Forschungsgemeinschaft Cluster of Excellence Ruhr Explores Solvation, RESOLV) and the European Research Council (Early Stage Organocatalysis, ESO) to B.L.

Author contributions:

Conceptualization: B.L., C.K.D.

Methodology: S.D, C.Z., C.K.D.

Investigation: S.D, C.Z., C.K.D.

Project administration: C.K.D., B.L.

Supervision: B.L.

EPR: D.D., B.E.

Writing – original draft: S.D.

Writing – review & editing: S.D, C.Z., C.K.D., B.L.

Competing interests: A patent WO2017037141 (A1) filed by the Max-Planck-Institut für Kohlenforschung and B.L. covers the IDPi catalyst class and its applications in asymmetric synthesis. The other authors declare no competing interests.

Data and materials availability: All data, code, and materials used in the analysis are available in supporting information.

Supplementary Materials

Materials, Methods and Supplementary Text